Kinks in a Lattice of Repelling Particles

Experimental Study with a Chain of Coupled Pendulums

Ahmed Mehrem, Luis J. Salmerón-Contreras, Noé Jiménez, Víctor J. Sánchez-Morcillo, Rubén Picó, Luis M. García-Raffi, Juan F. R. Archilla and Yuriy A. Kosevich

Abstract A lattice of repelling particles is a good model for studying certain properties that take place at atomic scale in Solid State Physics. In this chapter

A. Mehrem · V. J. Sánchez-Morcillo · R. Picó
Instituto de Investigación para la Gestión Integrada de las Zonas Costeras, Universitat Politècnica de València, C/.Paranimfo 1, 46730 Grao de Gandia, Spain
e-mail: ahmeh@epsg.upv.es

V. J. Sánchez-Morcillo
e-mail: victorsm@upv.es

R. Picó
e-mail: rpico@upvnet.upv.es

L. J. Salmerón-Contreras · L. M. García-Raffi (✉)
Instituto Universitario de Matemática Pura y Aplicada, Universitat Politècnica de València, Camino de Vera s/n, 46022 Valencia, Spain
e-mail: luisalco@epsg.upv.es

L. M. García-Raffi
e-mail: lmgarcia@mat.upv.es

N. Jiménez
LUNAM Université, Université du Maine, CNRS, LAUM UMR 6613 Av. O. Messiaen, 72085 Le Mans, France
e-mail: noe.jimenez@univ-lemans.fr

Present Address:
N. Jiménez
Instituto de Instrumentación para Imagen Molecular, Consejo Superior de Investigaciones Científicas, Universitat Politècnica de València, Camino de Vera s/n, 46022 Valencia, Spain
e-mail: nojigon@upv.es

J. F. R. Archilla
Group of Nonlinear Physics, Department of Applied Physics I, Universidad de Sevilla, ETSII, Avda Reina Mercedes s/n, 41012 Sevilla, Spain
e-mail: archilla@us.es

Y. A. Kosevich
Semenov Institute of Chemical Physics, Russian Academy of Sciences, Kosygin Street 4, 119991 Moscow, Russia
e-mail: yukosevich@gmail.com

© Springer International Publishing AG 2018

J. F. R. Archilla et al. (eds.), *Nonlinear Systems, Vol. 2*, Understanding Complex Systems, https://doi.org/10.1007/978-3-319-72218-4_11

we study theoretically and experimentally the generation and propagation of kinks in such kind of systems. We propose a simple experimental setup consisting in an array of pendulums, having magnets at the extreme, i.e., that form a set of coupled magnetic dipoles. We excite pulses at one boundary of the system and demonstrate the existence of transient-kinks, whose dynamics are in very good agreement with the theoretical predictions given by the α-FPU equation. The peculiarities of the experimental system allows to study a broad range of phenomena. On one hand, by the effect of the finite size of the magnets, the model captures the dynamics of different inverse power law inter-particle interactions, ranging from the monopole limit to the dipole interaction. On the other hand, we propose the use of an external substrate potential at the bottom of the lattice that mimics the substrate potential of a crystal. Thus, the results obtained in the experimental setup can be extrapolated to other systems described by this equation.

Keywords Repulsive forces · Magnetic pendula · Kinks

1 Introduction

Matter is formed by basic units, atoms, that interact via repulsive forces and form ordered states called lattices. These repulsive forces are the results of Coulomb interactions and short range repulsive forces due to the Pauli exclusion principle of many body systems [13]. Therefore, the study of such kind of systems from different points of view gives an insight to the properties of solid state physics, the part of physics that describes atoms and ions organized in ordered lattices called crystals. We are dealing with non-contact forces that provide the coupling between neighboring particles, fixed in some positions or sites by the potential of the rest of the lattice in the mean field approximation. This coupling allows the propagation of perturbations in the form of phonons, or elementary excitations of the lattice. But we are not restricted to work at atomic scale to find in nature examples of such kind of systems and coupling among entities. For example, in Ref. [24] it is presented a system of trapped interacting particles that form an ionic crystal. Such crystals – that can be considered as a particular form of condensed matter- are formed by charged particles confined by external electromagnetic potentials (Paul or other traps) [24], and interacting by means of the Coulomb repulsion. The process of crystallization requires a lowering in temperature that is achieved by laser cooling techniques. Different crystallization patterns have been observed by tuning the shape and strengths of the traps. Crystals of trapped ions have been subject of great attention as a possible configuration to perform quantum computation [23]. Crystallization of a gas of confined electrons, known as a Wigner crystal, has also been predicted and observed [8, 16].

When these systems are perturbed at their boundaries, waves propagate through them and due to the lattice periodicity strong dispersion appears when wavelengths are of the order of the lattice period. The linear dispersion relation for low amplitudes and some nonlinear characteristics of wave propagation have to be determined in

order to characterize wave propagation. For example, it has been experimentally determined in an electrically charged, micrometer-sized dust particles immersed in the sheath of a parallel plate rf discharge in helium in a rf plasma [10], where the waves are excited by transferring the momentum from a laser to the first particle in the chain. One of the effects that appear due to the nonlinearity of interparticle interactions is the generation of harmonics.

But this is not the only case of perturbation of the propagation we can study. In charged-coupled lattices of particles there is another *bestiarium* formed as a consequence of the excitation of intense compact pulses at one boundary of the system, giving rise to solitons, breathers, kinks, quodons, crowdions... All of them are solutions of the equations that govern the dynamics of the system based on the nonlinear character of the interactions and they behave as particle-like perturbations traveling along the lattice.

In recent decades, the solitary wave theory has become a very active area of research due to its importance in many branches of mathematics and physics, such as nonlinear optics, acoustics, plasmas and fluid mechanics. In particular, kinks have been extensively studied during the recent years because they transport energy at supersonic speeds [2–4]. In ionic crystals kinks are also natural carriers of electric charge [6]. One example of this kind of materials is mica muscovite. The tracks are recorded within the cation layer of potassium ions which form a two-dimensional hexagonal lattice. Some of these tracks can be explained by the passage of swift particles as positrons, pions, antimuons and protons which are secondary particles to neutrino collisions or products of radioactive decay. But there are also many tracks along the close packed directions of this lattice that cannot be produced by charged particles and are attributed to some vibrational entities called *quodons* because of their quasi one-dimensional character [1]. Their existence has also been shown experimentally in [26]. These *quodons* are triggered by the radioactive disintegration of potassium isotopes where the recoil of the nucleus in some cases has the necessary energy to start the propagation of a perturbation that travels along a lattice direction formed by a chain of potassium ions that lies in the (001)-plane [5].

Many studies have been done about kink propagation in different media [14, 18, 25]. Peyrard et al. [20] described and discussed subsonic kinks in a monoatomic chain where they showed the discreteness effects on non-topological kink soliton dynamics in nonlinear lattices. Savin et al. [28] studied moving topological solitons (kinks and antikinks) in the nonlinear Klein-Gordon chain by using the pseudo-spectral method. Pnevmatikos, Flytzanis and Remoissenet [21] studied propagation of kinks and solitons analytically and numerically in a nonlinear diatomic chain with cubic and quartic interaction potential. The book *"Waves called solitons: concepts and experiments"* by Remoissenet [25] describes examples of many simple experimental realizations of nonlinear lattices in which kinks, in particular, can be observed.

In this work we pay attention to lattices of nonlinear oscillators coupled to the nearest neighbours by repulsive interactions. Specifically, we study a 1D chain of particles periodically distributed that interacts via repulsive Coulomb-type forces. Our purpose is the experimental study of kinks in a mechanical analogue of a chain

of repulsive particles: a chain of magnetically coupled pendulums. The system is analogous to that of [27], but here, in addition to the action of gravity, a magnetic substrate potential was added, i.e., making a mechanical analogue of the Frenkel–Kontorova model. The modeling of repulsive interactions with finite-size magnetic dipoles allows the experimental study of different functions for the repulsive interaction. We study the excitation and propagation of kinks with and without the substrate potential, and compare the experimental results with analytical and numerical ones. Good agreement was obtained, showing that it is possible to build up and measure certain properties in simple macroscopic analogues of microscopic systems.The theoretical results are based in the work [12] and the experimental results have been obtained from the work [17].

2 The Physical Model

Our theoretical model consists of an infinite chain of identical particles with mass m aligned along the x-axis. Each particle interacts with its nearest neighbors via a repulsive potential, V_{int}. In the absence of perturbations, every mass has a fixed equilibrium position being the interparticle distance a. An external potential, V_{ext}, can be added to the lattice. In condensed matter, this external potential comes from the action of the other atoms or ions in the crystal. These extra forces can be provided by a periodic on-site potential and/or forces keeping the boundary particles at fixed positions. Then, the equation of motion is written as

$$M\ddot{u}_n = V'_{\text{int}}\left(u_{n+1} - u_n\right) - V'_{\text{int}}\left(u_n - u_{n-1}\right) - V'_{\text{ext}}\,, \tag{1}$$

where u_n represents the displacement of the n-th particle measured with respect to its equilibrium position as shown in Fig. 1, M is the mass of the particle and V'_i is the derivative of the potential V_i. Therefore, the rhs of the equation is the sum of the forces on the particle n by the nearest neighbors at $n+1$ and $n-1$ and by a substrate potential which can be produced by the rest of the lattice or an external cause. In the limit of small displacements, the interaction force between particles can be approximated linearly with respect to the distance, r, i.e., $V'(r) = \kappa r$ where κ is

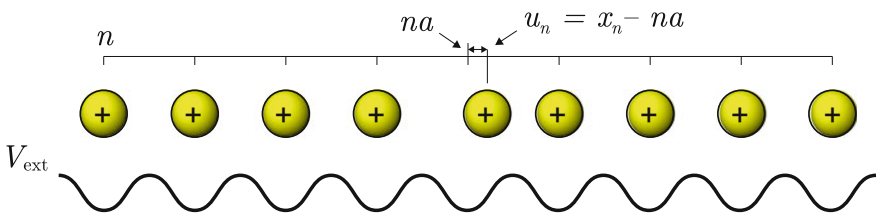


Fig. 1 The lattice of repelling coupled particles. The lattice constant is a. An external force applied in the boundaries is necessary to keep the system stable

a constant. In this limit, Eq. (1) represents a system of coupled harmonic oscillators. However, in general the potentials in physical systems are anharmonic. Chains of nonlinearly coupled oscillators with different types of anharmonic potentials have been extensively studied in the past, e.g., the celebrated cases of the α-FPU lattice, where $V'_{\text{int}}(r) = \kappa_1 r + \kappa_2 r^2$ (cubic potential), the β-FPU lattice where $V'_{\text{int}}(r) = \kappa_1 r + \kappa_3 r^3$ (quartic potential), the Toda lattice, with $V'_{\text{int}}(r) = \exp(-r) - 1$ or the granular lattice, with $V'_{\text{int}}(r) = \kappa r^{3/2}$.

In this work, we consider interparticle forces that decrease with an inverse-power law of the distance. The equation of motion for the particle n is then written in the form:

$$\ddot{u}_n = -\frac{1}{(1 + u_{n+1} - u_n)^\alpha} + \frac{1}{(1 + u_n - u_{n-1})^\alpha} - V'_{\text{ext}}\,, \tag{2}$$

The particular value of the exponent α bring us different types of interactions: $\alpha = 2$ corresponding to repulsive monopoles as in the case of electrically charged particles, e.g. in ion coulomb crystals [24] or dusty plasma crystals [19], $\alpha = 4$ corresponding to repulsive dipoles, e.g., in the interaction between distant magnetic dipoles [27], or in general any other non-integer power [18]. In the following, we present a system allowing to model different values of the exponent of the power-law, α.

3 The Lattice of Repelling Magnets

First, consider two magnetic dipoles, with magnetic moments $\mathbf{m}_1$ and $\mathbf{m}_2$. The interaction potential energy between them is given by the exact relation [11]:

$$V_{\text{int}} = \frac{\mu_0}{4\pi}\left(\frac{\mathbf{m}_1 \cdot \mathbf{m}_2}{r^3} - 3\frac{(\mathbf{m}_1 \cdot \mathbf{r}_{12})\,(\mathbf{m}_2 \cdot \mathbf{r}_{12})}{r^5}\right), \tag{3}$$

where $\mathbf{r}_{12}$ is the vector joining the centers of the dipoles, i.e., from the magnet 1 to the 2, and $r = |\mathbf{r}_{12}|$. This relation implies that, in general, the force depends on the angle between the dipoles. In the particular case when the dipole moments are equal in magnitude, parallel to each other and perpendicular to $\mathbf{r}$ (dipoles in the same plane), the force on the second magnet takes the simpler form

$$\mathbf{F}_{1,2} = -\nabla_2 V_{\text{int}} = \frac{3\mu_0}{4\pi}\frac{m^2}{r^4}\hat{r}_{12}, \tag{4}$$

where $m = |\mathbf{m}_1| = |\mathbf{m}_2|$, μ_0 is the permeability of the medium and $\hat{r}_{12}$ is the unitary vector in the direction from the center of magnet 1 to the center of magnet 2. The force on the first magnet is just the opposite. In the chain of magnetic dipoles, this is the force between two neighboring oscillators at equilibrium positions, i.e., with $r = a$.

In the case of the perturbed chain the distance between centers of nearest neighbors becomes a dynamic variable, $r_n(t)$. Assuming small displacements, i.e., a small angle between the dipole moments, we can use $r_{n+1}(t) = a + u_{n+1} - u_n$ in Eq. (4) to describe the interaction between two neighboring oscillators. The modulus of the force on the $n+1$ magnet due to the n magnet is

$$F_{n,n+1} = \frac{3\mu_0 m^2}{4\pi} \frac{1}{(a + u_{n+1} - u_n)^4} \,. \tag{5}$$

This equation for the small-angle forces is a crude approximation and exact expressions can be found in Ref. [27]. However, since our aim is to obtain simple analytical expressions based on the FPU equation, Eq. (9), we will keep this degree of accuracy. The validity of this approximation to describe our setup will be tested in the next sections when the predictions are compared with the experimental results. Comparing with the equation of motion shown in Eq. (2), we identify $\alpha = 4$.

The above expressions for the forces between magnetic dipoles are valid for loop currents or magnets of negligible dimensions. Expressions for finite size magnets can be found in the literature [7] and are in general lengthy and cumbersome. Gilbert's model for the magnetic field of magnets used here results in approximate but simple expressions for the forces [9]. For cylindrical magnets of length h with their magnetic moments parallel and their axis perpendicular to the line joining the centers, the force on magnet 2 due to the adjacent magnet 1 is expressed as

$$\mathbf{F}_{1,2} = \frac{\mu_0 m^2}{2\pi h^2} \left(\frac{1}{r^2} - \frac{r}{\left(r^2 + h^2\right)^{3/2}} \right) \hat{r}_{12} \,, \tag{6}$$

where the magnetic moment is $m = \pi h R^2 \mathrm{M}$, being M the magnetization and R the radius of the cylindrical magnet.

In the limit $h \ll r$, Eq. (6) reduces to Eq. (4), i.e. magnets with small dimensions compared to their separation interact via dipolar forces, i.e., $\alpha = 4$. In the opposite limit $h \gg r$, the interaction law approaches to a Coulomb-type force, i.e., $\alpha = 2$ for parallel magnets close to each other. In general, the interaction law of magnets can be approached well by an inverse-law with any given exponent that ranges between monopole and dipole cases. Therefore, the chain of repelling magnets allows the modeling of different physical situations just by adequately choosing the geometry of the system.

Thus, we built a chain of coupled magnets as a mechanical analogue of our lattice of particles coupled by repulsive forces. The experimental setup is shown in Fig. 2. An analogue experimental system was presented by M. Russell [27]. The chain consists of 53 identical cylindrical neodymium magnets (Webcraft GmbH, DE, magnet type N45), with mass $M = 2$ g, arranged in a one-dimensional periodic lattice. The radius and length of the magnets was $R = 2.5$ mm and $h = 14$ mm, respectively. The magnets were oriented with the closest poles being those of the same polarity, therefore producing a force that is repulsive. The value of the magnetization

was $\text{M} = 1.07 \times 10^6$ A/m. The magnets were attached to a rigid bar which allows the rotation in the sagittal plane around a fixed T-shaped support, being each magnet actually a pendulum as shown in Fig. 2b. The length of the vertical bars was $L = 100$ mm, and the lattice constant, i.e., the distance between supports (and therefore the distance between magnets at equilibrium) was $a = 20$ mm. The support was specially designed to minimize the effects of friction by using additional pairs of concentric rings magnets which keep the oscillators levitating on air, with just one contact point, as shown in Fig. 2c. This system allows the minimization of the friction: strong torque forces appear at the bearings of the pendulums due to non perfect alignment. Using the quasi-levitation system the chain remains aligned to one single axis, the losses are negligible and, therefore, the experimental setup can be considered quasi-conservative.

The effect of each pendulum is to introduce an additional external force to the dynamics of the chain, corresponding to $-V'_{\text{ext}}$ in Eq. (2).The restoring potential due to gravity is $V_{\text{ext}} = MgL(1 - \cos\theta_n)$, being θ_n the angle formed by a magnet with respect to its vertical equilibrium position and $u_n = L\sin(\theta_n)$ is the horizontal displacement variable. For small θ_n, $u_n \simeq L\theta_n$ and the potential becomes $V_{\text{ext}} \simeq \frac{1}{2}MgL\theta_n^2 = \frac{1}{2}M\Omega_0^2 u_n^2$ with $\Omega_0 = \sqrt{g/L}$ the frequency of small oscillations. The force on the pendulum n is then approximated by a linear force $F_{\text{ext}}(u_n) = -V'_{\text{ext}}(u_n) = -M\Omega_0^2 u_n$. For small oscillations, the interaction potential between two magnets at $n+1$ and n becomes also harmonic $V_{\text{int}}(u_{n+1} - u_n) = \frac{1}{2}\kappa(u_{n+1} - u_n)^2$ for some coupling constant κ.

All magnets oscillate freely except the outermost boundary magnets. The last magnet was fixed, and the first one was attached to the excitation system. The driving

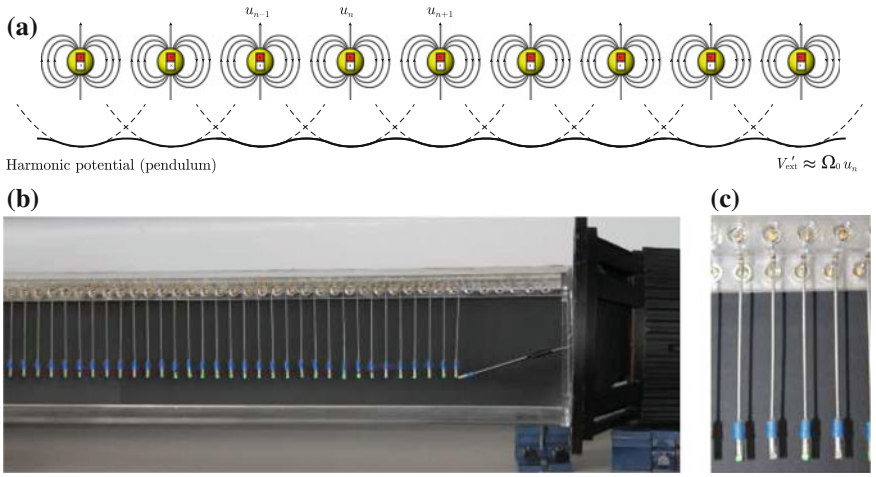


Fig. 2 **a** Scheme of the lattice of coupled particles with the harmonic restoring force. **b** The experimental setup: an array of pendulums, having magnets at the extreme, that form a set of coupled magnetic dipoles. **c** A detail of the concentric rings magnets which keep the oscillators levitating on air with only one contact point. Reproduced from [17]. Licensed under CC-BY-NC-ND

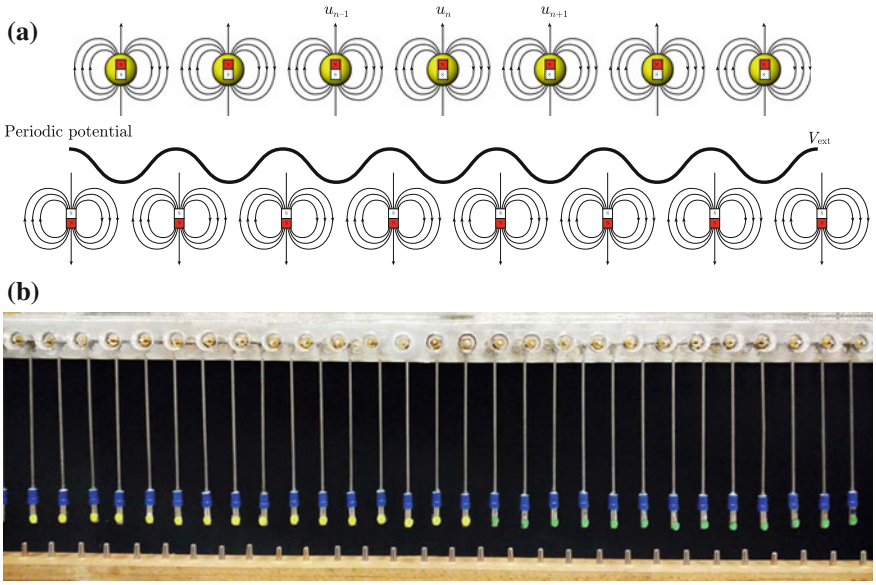


Fig. 3 **a** The scheme of the chain with added periodic substrate. The force between chain magnets and substrate magnets is repulsive. **b** The experimental setup showing on the top the moving-pendulum magnets and in the bottom the fixed-substrate magnets. Reproduced from [17]. Licensed under CC-BY-NC-ND

system consisted of a electrodynamic loudspeaker (Fostex-L363) connected to an audio amplifier (Europower EPS2500) excited by an arbitrary function generator (Tektronix AFG-2021). The first magnet was fixed to the loudspeaker's diaphragm as shown in Fig. 2, and it was forced with different pulsed excitations using a specific waveform with variable amplitude. The motion of the chain was recorded by using a GoPro-Hero3 camera. The camera was placed at proper distance from the chain in order to track the motion of a certain number of magnets. In this work, 18 magnets were recorded simultaneously. Then, each pendulum was optically tracked using image post-processing techniques. We considered the traveling wave regime, by ignoring the reflected wave using a temporal window in the analysis of the recorded video. The duration of each record was about 3.5 s and the camera resolution was set to 960p at a frame rate of 100 frames per second, i.e., a sampling frequency of 100 Hz for the measured displacement waveforms. Videos were post-processed with Matlab using standard image tracking techniques to detect the movement of the magnets obtaining finally a waveform for the position of each magnet.

In this system we have studied the propagation of kinks under two different configurations:

1. **Harmonic substrate potential**: In the first configuration, a weak harmonic potential is introduced due to the restoring force of the pendulum as shown in Fig. 2a. The length of the pendulums was designed to present a small resonating fre-

quency and, therefore, V'_{ext} is extremely weak if compared to the repulsive forces between magnets. However, the existence of the pendulum introduces a restoring force and the unique stable state corresponds to $u_n = 0$. As we will show, this has implications in the formation of kinks.

2. **Periodic substrate potential**: In the second case, a set of fixed magnets were added at the bottom of the chain, as shown in Fig. 3, being each fixed magnet at a distance of 15 mm to the chain and with the polarity vertically inverted with respect to the moving-magnets. The dimensions of the fixed NdFeB magnets were $R_{\text{fix}} = 4$ and $h_{\text{fix}} = 12.5$ mm with same magnetization as the moving ones (Webcraft GmbH, DE, magnet type S-04-13-N). All magnets were placed on non-magnetic support to prevent any interaction with the magnetic field produced by the system. The effect of this extra magnetic repulsive field is that, in addition to the weak restoring gravity forces, it produces strong repulsive magnetic forces, introducing a strong periodic substrate potential, V_{ext}, if compared to the repulsive forces between magnets. The inclusion of this substrate introduces periodic restoring forces with multiple stable states as $u_n = \pm n$: the oscillators can be at rest at different lattice positions. The situation is represented in Fig. 3a.

Thus, just by modifying the geometry of the system, e.g. the distance between the substrate magnets to the chain, the intensity of V'_{ext} can be modified, allowing the current experimental setup to be a mechanical analogue of different nonlinear lattices, ranging from the FPU lattices to the Frenkel–Kontorova ones.

4 Dispersion Relations

The dispersion relation of the lattice is derived for small amplitude waves. It can be obtained analytically by using the Taylor expansion of the α power law in the equation of motion Eq. (2), neglecting the nonlinear terms and assuming a solution in the form of $u_n = \exp[i(\omega t - qn)]$, where q is the wave number and ω is the angular frequency. Then, the dispersion relation is written as

$$\omega^2 = \omega_0^2 + \omega_c^2 \sin^2\left(\frac{q}{2}\right), \tag{7}$$

where ω_0 is the lower cut-off frequency, and $\omega_c = 2\,c_0$, with $c_0^2 = \kappa/M$, where κ is the coupling constant, being a measure of the stiffness of the interaction potential. If there is no substrate potential, i.e., $\omega_0 = 0$, the phonon frequencies are not bounded from below, and the dispersion relation is called *acoustic*. In this case c_0 is the sound phase and group velocity, that is, the velocity for the long-wavelenght limit $q \to 0$ and the maximum frequency becomes $\omega_c = 2\,c_0$, being therefore a *coupling frequency*. For the system of interest in this chapter, $\omega_0 \neq 0$, the phonon frequencies are bounded from below and the dispersion relation is called *optical*, the highest cut-off frequency becomes $\omega_{\text{top}} = (\omega_0^2 + \omega_c^2)^{1/2}$. Figure 4 shows the dispersion relation for the two configurations, with weak and strong substrate potential. It can be

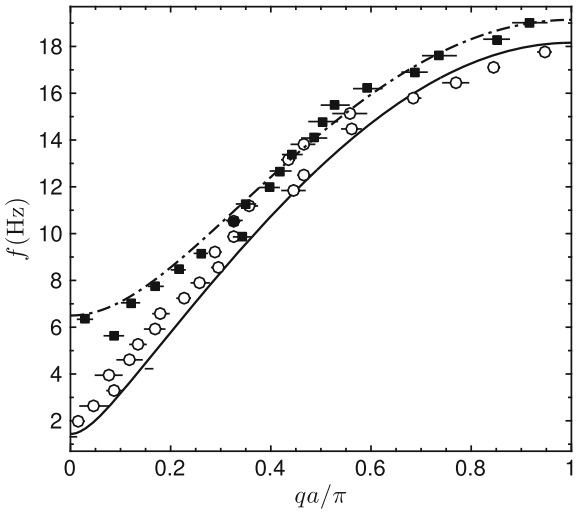


Fig. 4 Dispersion relation in case of the setup with/without substrate. (line-Dashed) Analytically presented by Eq. 7 $\omega^2 = \omega_0^2 + \omega_c^2 \sin^2(q/2)$. The frequency in Hz is given by $f = \omega/2\pi$. The experimental data with error bars (circles) for the case with weak harmonic substrate potential and (squares) for the case with stronger periodic substrate potential. Analytical results are represented by the continuous line for the weak harmonic substrate potential and $(- \cdot -)$ for the stronger periodic substrate potential. Reproduced from [17]. Licensed under CC-BY-NC-ND

observed the existence of high and low cut-off frequencies: both dispersion relations are optical. For the weak substrate potential case, the low cut-off frequency is $\omega_0 = \sqrt{g/L}$ where L is the pendulum length and the gravitational acceleration $g = 9.8\,\mathrm{m/s^2}$. In the case of the strong substrate potential, the low cut-off can be evaluated by measuring the forces of the magnetic dipoles along the axis of the chain. However, for cylindrical magnets of finite dimensions it can become cumbersome and it was estimated experimentally from the dispersion relations. In particular, in the case of the unique action of the gravity (weak substrate potential) the low cut-off frequency presented a value corresponding to $f_0 = \omega_0/2\pi = 1.6\,\mathrm{Hz}$. In the second case, with the strong substrate potential, it was increased up to 6.5 Hz. The high cut-off frequencies were respectively 18 and 19.1 Hz. In Fig. 4 we present the experimental data together with the solution given by Eq. (7) where the values ω_0 and c^2 were set to the corresponding experimental values in each case. A good agreement between the experiments and the theoretical curves is observed. Then, this system presents strong dispersion arising from the two sources, first, the lattice discreteness and, second, the substrate potential, that can be easily tuned by the modification of the geometry of the proposed setup.

5 Approximate Analytical Solution

It is well-known that the interaction of strong dispersion and nonlinearity of a system leads to the emergence of nonlinear localized traveling waves. However, Eq. (2) has no analytical solution. Therefore, we present approximate analytical solutions that capture the main dynamical features of the lattice, in particular, looking for solution of kinks. Approximate solutions can be obtained assuming a small strain $|u_{n\pm1} - u_n|$ in comparison with the lattice constant a. Under this approximation the equation of motion reduces to the well-known FPU equation. Using the FPU equation many solutions for nonlinear localized waves have been proposed in the past. Kosevich [14] obtained a model based on a FPU equation with a cubic plus quartic nonlinearity. Poggi and Ruffo [22] derived an exact solution of the FPU corresponding to Lennard-Jones interaction forces. Recently, Archilla, Kosevich et. al [3] obtained the FPU equation for a cubic plus quartic nonlinearity from the expansion of the Coulomb potential. In all these cases, the authors relied on a FPU equation to extract analytical solutions for kinks. For a weak substrate potential, Eq. (2) is a generalized form of the equation of motion presented by Archilla et al. [4]. Replacing the forces by their Taylor expansion and neglecting cubic and higher order terms, the leading equation in the general case of a inverse power law is

$$\ddot{u}_n = c_0^2 \left[(u_{n+1} - 2u_n + u_{n-1}) - \frac{1+\alpha}{2} (u_{n+1} - u_n)^2 + \frac{1+\alpha}{2} (u_n - u_{n-1})^2 \right] - \Omega_0^2 u_n, \quad (8)$$

where $c_0 = \sqrt{\alpha}$ is the normalized long wavelength phonon velocity in the absence of substrate, i.e., the speed of sound. In the case of monopolar interaction ($\alpha = 2$) it leads to

$$\ddot{u}_n = c_0^2 \left[(u_{n+1} - 2u_n + u_{n-1}) - \frac{3}{2} (u_{n+1} - u_n)^2 + \frac{3}{2} (u_n - u_{n-1})^2 \right] - \Omega_0^2 u_n, \quad (9)$$

and for dipolar interaction, $\alpha = 4$, the FPU takes the form

$$\ddot{u}_n = c_0^2 \left[(u_{n+1} - 2u_n + u_{n-1}) - \frac{5}{2} (u_{n+1} - u_n)^2 + \frac{5}{2} (u_n - u_{n-1})^2 \right] - \Omega_0^2 u_n \,. \quad (10)$$

This equations show that the nonlinearity for the case of dipolar interaction is increased, with respected to the monopolar interaction.

The on-site potential restoring force $-V'_{\text{ext}}$ is in general a nonlinear function. However, for small displacements, as considered here, it can be linearized as $-V'_{\text{ext}} = -\Omega_0^2 u_n$, where Ω_0 is the normalized frequency of oscillation of a particle due to the external potential. If the on-site potential term is neglected (no external forces acting on the chain), Eq. (9) reduces to the celebrated α-FPU equation.

Following our purpose of obtaining approximate analytical solutions that describe the main dynamical features of our system, let us neglect the weak on-site potential term. Defining the strain as $v_n = u_n - u_{n-1}$, we obtain the motion equation of the

strain for $\alpha = 2$ as

$$\ddot{v}_n = -\frac{1}{(1+v_{n-1})^2} + \frac{2}{(1+v_n)^2} - \frac{1}{(1+v_{n+1})^2}\,, \tag{11}$$

where $v_n = 0$ corresponds to an unperturbed bond. Kinks can be excited by forcing the lattice with a half-wave perturbation. That can be done producing a sinusoidal displacement of the particle at one of the boundaries during half of the period that returns to the equilibrium position after finishing the pulse. For describing a kink profile traveling to the right, the following *ansatz* is introduced [14, 15]:

$$v_n = \begin{cases} -\frac{A}{2}\left[1+\cos\left(qn-\omega t\right)\right] & \text{if} \quad -\pi < \frac{2\pi}{3}n - \omega t < \pi \\ \\ 0 & \text{otherwise.} \end{cases} \tag{12}$$

where A represents the kink strain amplitude. The displacements of the particles in the lattice corresponds to compressed bonds, so v_n is a variable that takes negative values, being its maximum value $|v_n|_{\max} = A$ corresponding to the maximal compression of a bond. Looking at Eq. (12) we realize that for such a pulsed excitation q it is not strictly speaking the wavenumber and ω the frequency, but we will adopt this terminology for being the used one in the literature.

Equation (12) with $q = 2\pi/3$ is an exact solution of the $\alpha - \beta$ FPU lattice [15]. This particular value of q is known in the literature as the *magic wavenumber*. For a given wavenumber and taking into account the relation $\lambda = 2\pi/q$ we obtain solutions where an integer value of bonds (λ) and particles ($\lambda - 1$), i.e., the kink core, are in motion. The first case is the *magic wavenumber* $\lambda = 3$ ($q = 2\pi/3$) where 2 particles are moving at a given time. The other important mode correspond to $\lambda = 2$ ($q = \pi$), referred here and beyond as the π-mode, when only one particle is moving at a given time. This mode is the limit where only one particle is moving at a given time and it corresponds to a hard-spheres potential with zero radius. This is therefore a reference mode and real systems can only approximate it at high energies.

6 Harmonic Substrate Potential

6.1 Transient Kinks

Using the weak substrate potential configuration, as shown in Fig. 2a, experimental results were obtained driving the chain at the first oscillator with a pulsed waveform excitation (half-sinusoidal wave). The obtained temporal waveforms for the displacement and the compression are shown in Fig. 5a, b for a strain amplitude $A = 0.15$. This figure shows the experimental results using the magnetic chain and the numerical simulations using Eq. (2) with an inverse power law close to the dipole iteration

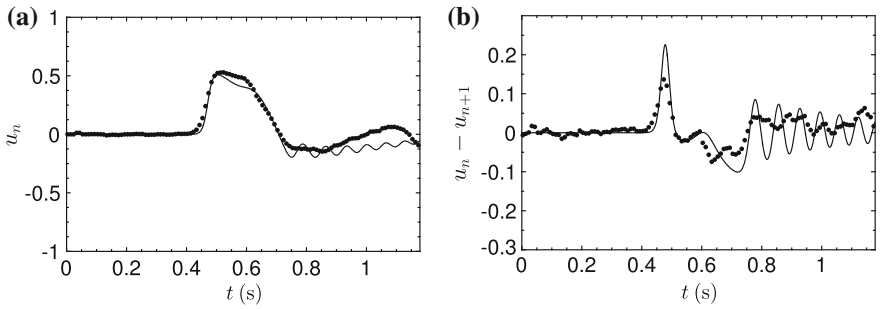


Fig. 5 **a** Kink profile in time, u_n, measured at $n = 23$. Numerical solution of Eq. (2) including the harmonic substrate (solid line), and experimental data (back dots). **b** Corresponding compression $-v_{n+1} = u_n - u_{n+1}$. Parameters $\alpha \simeq 3.6$ and approximate substrate harmonic potential with frequency $f_0 = \Omega_0/2/pi\,1.5\,\text{Hz}$

type, $\alpha = 3.6$, and a harmonic substrate potential with $f_0 = \Omega_0/2\pi = 1.5\,\text{Hz}$. The experimental data are in good agreement with the numerical simulation. It can be observed the formation of a kink at the front of the displacement wave (Fig. 5a), leading to a compression soliton as it is clearly observed in Fig. 5b. Then, after about 0.3 s, it can be seen the effect of the restoring force of the pendula: as the unique stable state is $u_n = 0$, the chain relaxes to its initial position and no exact kink can be formed. After the kink passes, a phonon tail is observed, being its arrival time given by the linear dispersion relations.

Although the kinks in a chain with a linear restoring force are not stable, the wavefront of these transient kinks obeys the analytical solution (12). The profile of the kink in space is shown in Fig. 6. Here, we show the numerical and experimental solutions, and the analytical solution of the FPU equation with $\alpha = 2$, i.e., Eq. (12). First, it can be observed that kinks can be excited in the experimental lattice for the temporal window analyzed. The experimental data are in good agreement with the numerical simulation and the analytic solution for a wavenumber $q \approx 2\pi/4$. The number of bonds in the numerical and analytical solutions can be obtained by fitting the profile to and it is $\lambda \approx 4.5$, while the number of particles in motion is $\lambda - 1 \approx 3.5$. Thus, in the experimental data, the number of bonds and number of particles in motion seem to increase from the magic wavenumber kinks $\lambda = 3$. This can be caused by the effect of the weak harmonic potential, the separation from the $\alpha - \beta$-FPU equation due to large displacements, and to the magnetic force, for which the long range interaction and the multiple neighbors interaction must be taken into account. Research on the subject is underway and will be published elsewhere [4].

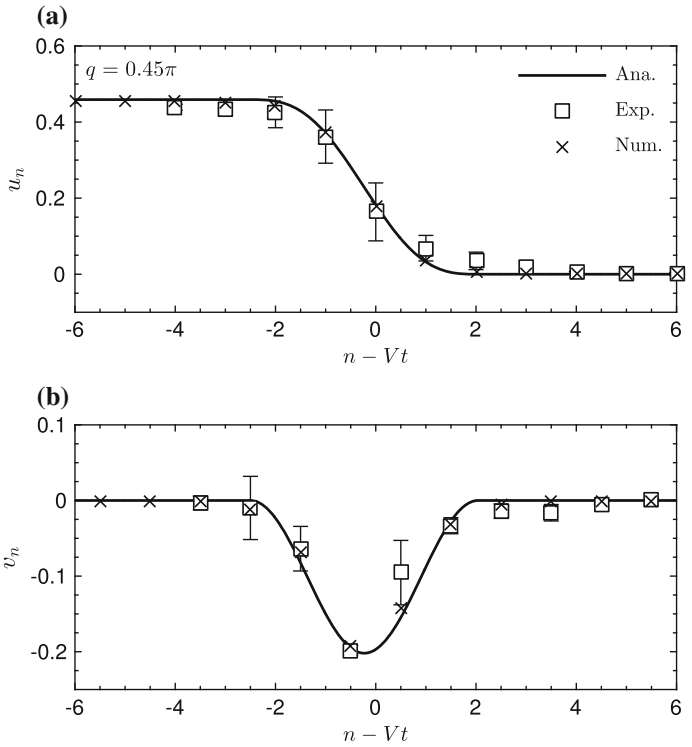


Fig. 6 **a** Kink profile in space, u_n, for pendulums ranging from $n = 23, 33$ of a chain of $N = 53$ magnets. Analytic solution using Eq. (12) $q = 2\pi/3$ (solid line), numerical simulation Eq. (2) (back dots), and experimental data (circles). **b** Corresponding strain $v_n = u_n - u_{n-1}$. Parameters $\alpha \simeq 3.6$ and approximate substrate harmonic potential with $f_0 = 1.5$ Hz. Reproduced from [17]. Licensed under CC-BY-NC-ND

6.2 *Kink Velocity*

The characterization of the kink velocity has been previously studied in Archilla et al. [2] where they used the Rotating Wave Approximation (RWA) to introduce the relation between the kink velocity V and the excitation amplitude A. When we substitute the *ansatz* of Eq. (12) into (11), we generate multiple terms with different frequencies. Following the RWA we select only terms up to the first harmonic, neglecting higher harmonics. We obtain the frequency ω as a function of the amplitude A as

$$\omega = \frac{1}{(1-A)^{3/4}} \omega_c \sin\left(\frac{q}{2}\right) , \tag{13}$$

where $\omega_c = 2c_0 = 2\sqrt{\alpha}$, and from this Eq. (13) we can calculate the kink velocity V as:

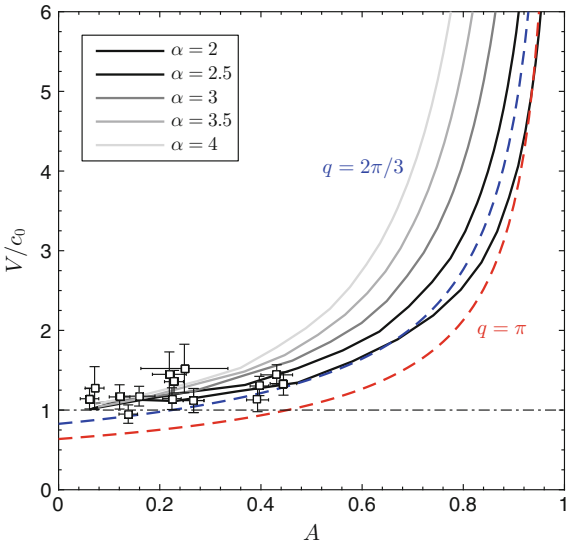


Fig. 7 Normalized kink velocity, V/c_0, versus kink amplitude, A. RWA solution $q = [\pi, 2\pi/3]$ (dashed lines), simulations of the chain for different inverse power laws (gray lines) and experimental data (markers). We tracked the pendula $n = 25, 26, 27$. Experimental data obtained with a weak harmonic potential and theoretical curves for a system without substrate as given by Eq. (14). Reproduced from [17]. Licensed under CC-BY-NC-ND

$$V = \frac{\omega}{q} = \frac{1}{(1-A)^{3/4}} \frac{2c_0}{q} \sin\left(\frac{q}{2}\right) . \tag{14}$$

Therefore, kinks are supersonic. Figure 7 shows the kink velocity V versus its amplitude A. Two cases are shown, first $q = \pi$ which means that only one particle is moving and *magic wavenumber* $q = 2\pi/3$ when two particles are in motion. The experimental results are also shown in Fig. 7 for a range of amplitudes ranging from $A = [0.07, 0.5]$. First, it can be seen that increasing the excitation amplitude makes the kink to propagate faster, being its speed always supersonic. Second, for the measured amplitude range, the experimental data for the transient kinks are compatible with the *magic wavenumber* $q = 2\pi/3$ solution and not with the π-mode as stated above. Third, the effect of the exponent of the inverse power law is to increase the sound speed in the system without substrate, which is $c_0 = \sqrt{\alpha}$. Finally, as can be clearly seen in the Taylor expansion of the FPU Eq. (8), increasing α at the particle interaction also increases the nonlinearity of the system. This leads to higher kink velocity values for the dipole interaction than for the purely Coulomb (monopole) interaction, being the family of supersonic solitons strongly dependent on the exponent of the inverse power law α.

6.3 Old Age Solution: Breathers

The kink solution is only valid for the initial transient. If the substrate potential V_{ext} introduces a linear restoring force with no periodicity in space, the unique stable

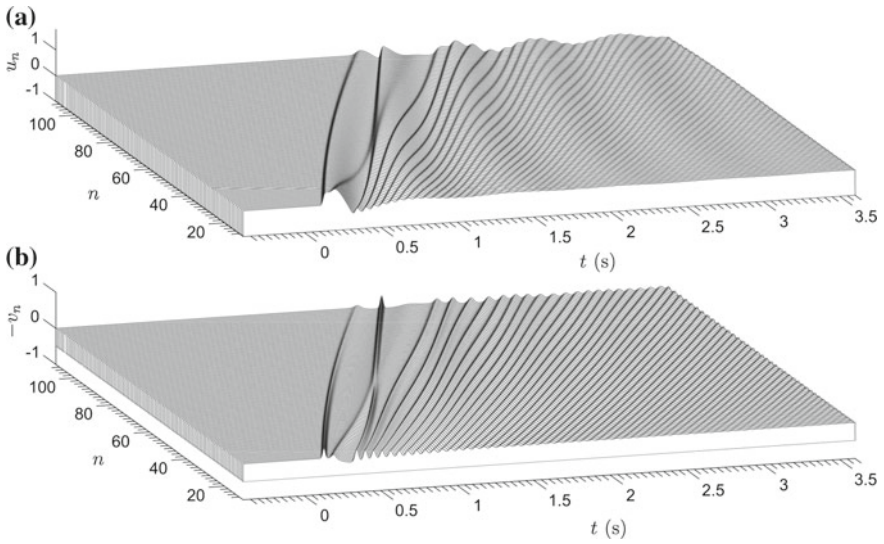


Fig. 8 Space-time profiles for transient solution. **a** Displacement and **b** compression $-v_n = u_{n-1} - u_n$ of the transient solution including a harmonic restoring force with characteristic frequency $f_0 = 1.5\,\mathrm{Hz}$

state is $u_n = 0$, and, therefore, the kink cannot be formed in the old-age solution. The transient process is shown in Fig. 8 for the displacement and for the compression $-v_n = u_{n-1} - u_n$ respectively. It can be observed that at the beginning of the chain the kink solution is similar to those obtained in the measurements. However, for longer distances the kink degenerates in other nonlinear waves. For old-age solution, we obtain other nonlinear localized excitation traveling at the kink front. The solution is shown in Fig. 9a–c for the dipole case, $\alpha = 4$. Simulations show that the nature of the dynamics of the system do not depend substantially on the exponent of the inverse power law. First, for a weak harmonic potential, similar to the effect of the pendula in the experiments, i.e. with a characteristic frequency of $f_0 = 1.5Hz$, we observe a large transient. Then, the kink disaggregates: the core of the kink transforms gradually into a breather-like localized state. The old-age solution is shown in Fig. 9a, where a stable localized nonlinear wave is observed and propagates at supersonic speed. This localized wave is internally composed of three internal solitonic oscillations that travel inside the core of the breather faster than the breather itself. Simulations show that this nonlinear localized mode is stable. Once formed, the breather composed by this three solitonic waves propagates thousand of lattice units.

The dynamics of these localized nonlinear waves is linked to the substrate potential. Figure 9b shows the space-time profile of the old-age solution for a different harmonic substrate with characteristic frequency of $f_0 = 3.5$ Hz. The transient from the kink to the breather is shortened, and also its width. Because of the shortening of the breather, its composing internal waves are more evident. Finally, the solution

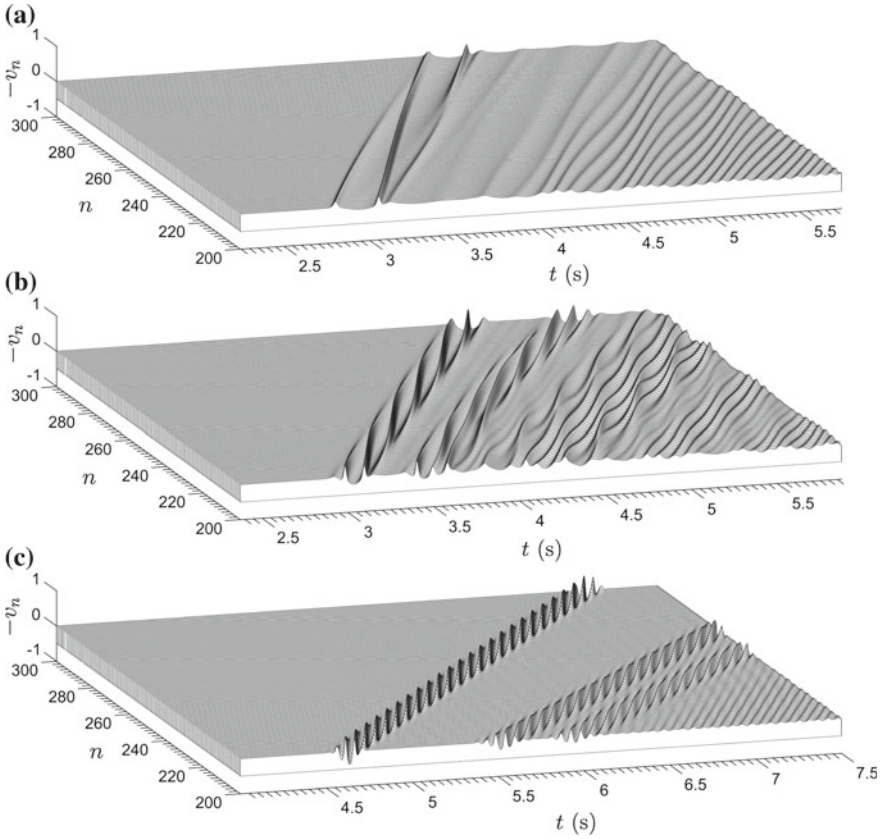


Fig. 9 Space-time profiles for the compression $-v_n = u_{n-1} - u_n$ of the old-age solution including a harmonic restoring force with characteristic frequencies of **a** $f_0 = 1.5$ Hz, **b** $f_0 = 3.5$ Hz and **c** $f_0 = 10$ Hz

including a high frequency substrate, $f_0 = 10$ Hz, is shown in Fig. 9c, where it can be observed that the breather frequency remarkably increased.

In this case, a single packet of energy propagates supersonically through the lattice. The localization also depends on the substrate potential and the strain amplitude of the localized wave, ranging from 22 lattices units for the low frequency substrate to 10 to the high frequency one. The internal dynamics shows that the core of the localized state is formed by three internal oscillations. The corresponding displacement is shown in Fig. 10a–c, where the localized waves are also clearly observed. After the wave passes, the harmonic potential force the lattice to oscillate around $u_n = 0$, therefore, no kink can be formed in the old-age solution.

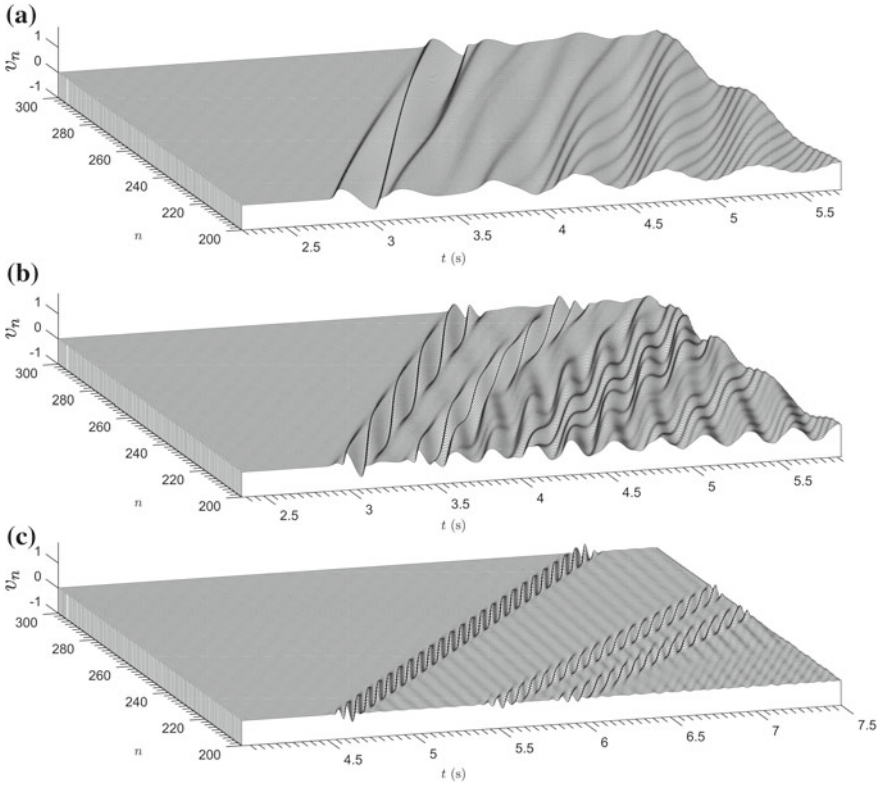


Fig. 10 Space-time profiles for the displacements v_n of the old-age solution including a harmonic restoring force with characteristic frequencies of **a** $f_0 = 1.5$ Hz, **b** $f_0 = 3.5$ Hz and **c** $f_0 = 10$ Hz

7 Periodic Substrate Potential

The experimental results previously shown were obtained including a weak on-site potential due to the gravity restoring force that brings pendulums to their equilibrium position in the chain. The smallness of this force compared to the magnetic repulsive interaction allows us to neglect the effect of the substrate potential for the transient solution observed in the experiments, i.e., the low cut-off frequency of the dispersion relation is near zero.

A more realistic model of condensed matter, with multiple stable states at $u_n = n$, can be obtained using the current experimental setup by including a strong and periodic substrate potential using the configuration shown in Fig. 3. A set of fixed magnets is placed periodically at $x = (n + 1/2)a$, being the vertical separation $h =$ 15 mm. The chain is excited under the same conditions than in the previous study. The simulated waveforms are shown in Figs. 11 and 12 for the strain and the displacement, respectively. First, it can be observed that with a periodic substrate force $V'_{\text{ext}} =$

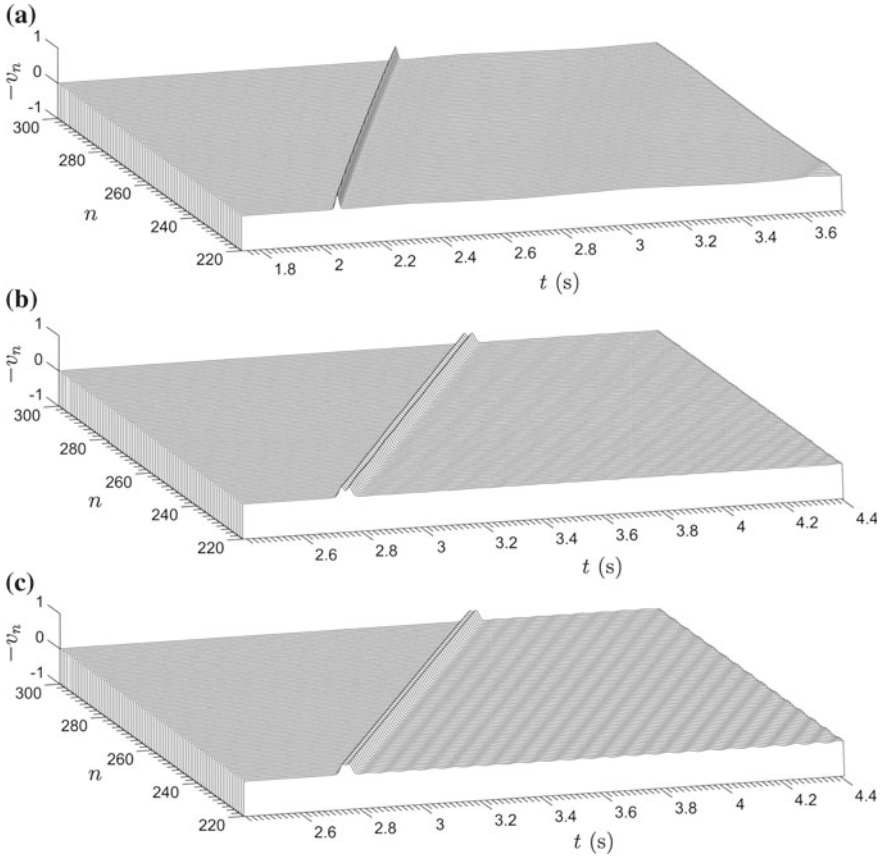


Fig. 11 Space-time profiles for the compression $-v_n = u_{n-1} - u_n$ of the old-age solution including a periodic restoring force with characteristic frequencies of **a** $f_0 = 1.5$ Hz, **b** $f_0 = 6.5$ Hz and **c** $f_0 = 10$ Hz

$\Omega_0^2 \sin 2\pi u_n$, with a characteristic frequency of $f_0 = \Omega_0/2/pi = 1.5$ Hz, a kink is formed that travels at supersonic speed, meaning at a speed both larger than the maximum group velocity of the phonons in the system with substrate, but also larger than the sound speed in the system without substrate. Behind the kink it is also observed a phonon radiation tail that oscillates at the characteristic frequency of the periodic substrate. It is worth noting here the strong differences in the dynamics of the nonlinear localized waves generated between systems using a harmonic restoring force or a periodic substrate potential, even when both small-amplitude frequency of the substrates are equal. If this frequency is increased, i.e., for stronger substrate potentials, the kinks are still observed, as shown for $f_0 = 6.5$ Hz in the space-time strain and displacement plots in Figs. 11b and 12b respectively, and in Figs. 11c and 12c for a strong substrate interaction with $f_0 = 10$ Hz. Here, the dynamics are essentially similar to the one obtained for a realistic potentials of mica muscovite in

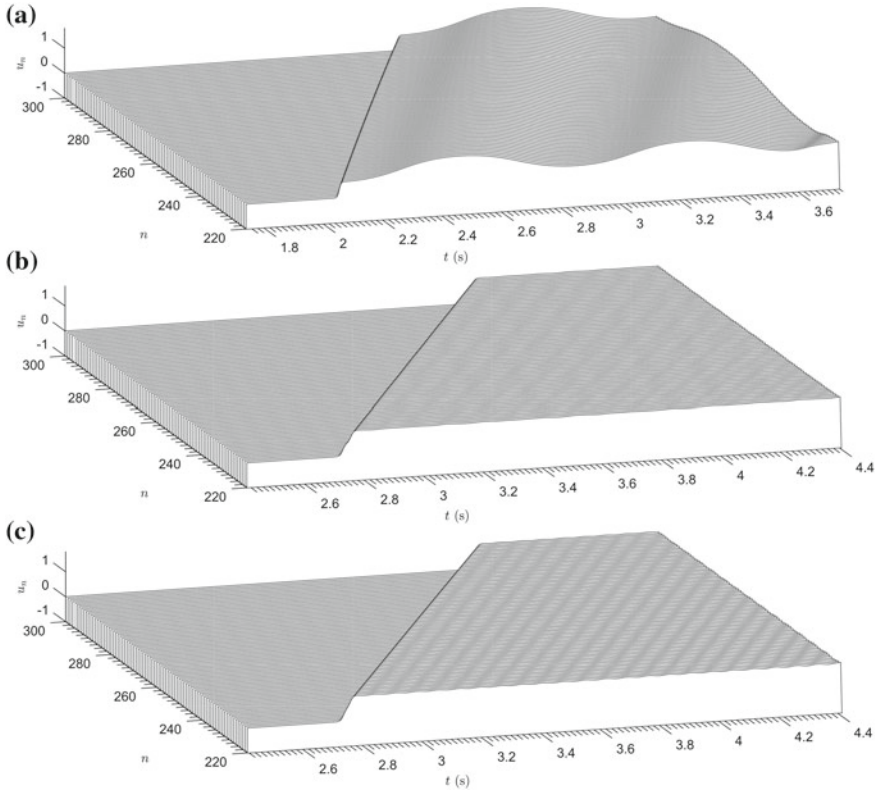


Fig. 12 Space-time profiles for the displacements u_n of the old-age solution including a periodic restoring force with characteristic frequencies of **a** $f_0 = 1.5$ Hz, **b** $f_0 = 6.5$ Hz and **c** $f_0 = 10$ Hz

Ref. [4], showing that the periodic substrate potential is a necessary factor to obtain stable kinks in latices.

8 Conclusions

Chains of particles coupled by repulsive forces allow the study of certain properties of condensed matter at a bigger scale. In particular, we have built a system of coupled pendulums that opens the possibility to perform experimental studies that at atomic scale become extremely difficult or unpractical. The study of such kind of systems have several advantages. The first one is that, after some assumptions, it is possible to approximate the corresponding equation of motion to the celebrated FPU equation, i.e., it allows us to obtain analytical approximate solutions. The second one is that

the complete equation is numerically integrable, giving a accurate approximation of the exact dynamics to guide the experiments.

In this chapter, we focus the study on kinks and localized nonlinear excitations in repulsive lattices with substrate potentials. Such type of system admits a mechanical analogue that can be studied in the laboratory and, exciting it conveniently, allows the study a broad range of nonlinear localized waves. In particular, we presented here a system consisting of a chain of repulsive oscillators coupled magnetically. The effect of the finite size of the magnets allows the modeling of different repulsive interactions, following all of them the inverse power law with the distance. Thus, just by modifying the geometry of the chain we can study repulsive interactions of monopolar (Coulomb type), dipolar or non-integer power type. Moreover, we have presented the dynamics that emerges from the different nature of the substrate potential.

If the substrate potential is purely harmonic, i.e., the restoring force is linear, as in the case of long pendulums, we show that kinks can exist only for a short time, and after a transient, supersonic breathers are formed. The dynamics of the system is deeply related with the fact that every pendulum is subjected to a restoring force, the gravity, for which the unique stable state corresponds to the displacement $u_n = 0$. The situation is completely different if we include a periodic substrate potential that allows multiple stable states in the chain. In this case, we report the generation of kinks that travel at supersonic speed through the lattice. It is worth noting here that in the chain of magnets a periodic substrate potential can be introduced simply by including a set of fixed magnets that adds repulsive periodic forces, much more intense than the corresponding to the restoring force due to gravity, i.e., that dominates the dynamics of the system.

Acknowledgements All authors acknowledge grant FIS2015-65998-C2-2-P from Ministerio de Economía y Competitividad (MINECO), Spain, which funded this research. AM gratefully acknowledge to Generalitat Valenciana (Santiago Grisolia program). LJSC gratefully acknowledge the support of PAID-01-14 at Universitat Politècnica de València. JFRA also aknowledges the (2017/FQM-280) grant from Junta de Andalucía.

References

1. Archilla, J.F.R., Jiménez, N., Sánchez-Morcillo, V.J., García-Raffi, L.M. (eds.): Quodons In Mica: Nonlinear Localized Travelling Excitations In Crystals, Springer series in materials science, vol. 221. Springer International Publishing, Cham (2015)
2. Archilla, J.F.R., Kosevich, YuA, Jiménez, N., Sánchez-Morcillo, V.J., García-Raffi, L.M.: Moving excitations in cation lattices. Ukr. J. Phys. **58**(7), 646–656 (2013)
3. Archilla, J.F.R., Kosevich, YuA, Jiménez, N., Sánchez-Morcillo, V.J., García-Raffi, L.M.: Supersonic kinks in Coulomb lattices. In: Carretero-González, R., Cuevas, J., Frantzeskakis, D., Karachalios, N., Kevrekidis, P.G., Palmero, F. (eds.) Localized Excitations in Nonlinear Complex Systems, pp. 317–331. Springer International Publishing, Cham (2014)
4. Archilla, J.F.R., Kosevich, YuA, Jiménez, N., Sánchez-Morcillo, V.J., García-Raffi, L.M.: Ultradiscrete kinks with supersonic speed in a layered crystal with realistic potentials. Phys. Rev. E **91**(2), 022912 (2015)

5. Archilla, J.F.R., Kosevich, Yu.A., Jiménez, N., Sánchez-Morcillo, V.J., García-Raffi, L.M.: A supersonic crowdion in mica. In: J.F.R. Archilla, N. Jiménez, V.J. Sánchez-Morcillo, L.M. García-Raffi (eds.) Quodons In Mica: Nonlinear Localized Travelling Excitations In Crystals, Springer Series in Materials Science, vol. 221, pp. 69–96 (2015)
6. Archilla, J.F.R., Russell, F.M.: On the charge of quodons. Lett. Mater. **6**, 3–8 (2016)
7. Camacho, J.M., Sosa, V.: Alternative method to calculate the magnetic field of permanent magnets with azimuthal symmetry. Rev. Mex. Fis. **59**, 8–17 (2013)
8. Deshpande, V.V., Bockrath, M.: The one-dimensional Wigner crystal in carbon nanotubes. Nat. Phys. **4**(4), 314–318 (2008)
9. Griffiths, D.J.: Introduction to Electrodynamics, 3 edn. Prentice Hall (2007)
10. Homann, A., Melzer, A., Peters, S., Piel, A.: Determination of the dust screening length by laser-excited lattice waves. Phys. Rev. E **56**(6), 7138–7141 (1997)
11. Jackson, J.D.: Classical Electrodynamics, 3 edn., p. 190 WileyJohn Wiley and Sons (1999)
12. Jiménez, N.: Nonlinear acoustic waves in complex media. Ph.D. thesis, Universitat Politècnica de València, València, Spain (2015). https://doi.org/10.4995/Thesis/10251/53237
13. Kittel, C.: Solid State Physics, 8 edn. John Wiley and Sons (2004)
14. Kosevich, YuA: Nonlinear sinusoidal waves and their superposition in anharmonic lattices. Phys. Rev. Lett. **71**(13), 2058–2061 (1993)
15. Kosevich, YuA, Khomeriki, R., Ruffo, S.: Supersonic discrete kink-solitons and sinusoidal patterns with magic wave number in anharmonic lattices. Europhys. Lett. **66**(1), 21–27 (2004)
16. Matveev, K.A., Andreev, A.V., Pustilnik, M.: Equilibration of a one-dimensional Wigner crystal. Phys. Rev. Lett. **105**(4), 046401 (2010)
17. Mehrem, A.: Nonlinear acoustics in periodic media :from fundamental effects to applications. Ph.D. thesis, Universitat Politècnica de València, València, Spain (2017). https://doi.org/10.4995/Thesis/10251/80289
18. Molerón, M., Leonard, A., Daraio, C.: Solitary waves in a chain of repelling magnets. J. Appl. Phys. **115**(18), 184901 (2014)
19. Nosenko, V., Avinash, K., Goree, J., Liu, B.: Nonlinear interaction of compressional waves in a 2D dusty plasma crystal. Phys. Rev. Lett. **92**(8), 085001 (2004)
20. Peyrard, M., Pnevmatikos, S., Flytzanis, N.: Discreteness effects on non-topological kink soliton dynamics in nonlinear lattices. Phys. D **19**(2), 268–281 (1986)
21. Pnevmatikos, St, Flytzanis, N., Remoissenet, M.: Soliton dynamics of nonlinear diatomic lattices. Phys. Rev. B **33**(4), 2308–2321 (1986)
22. Poggi, P., Ruffo, S.: Exact solutions in the FPU oscillator chain. Phys. D **103**(1–4), 251–272 (1997)
23. Porras, D., Marquardt, F., Von Delft, J., Cirac, J.I.: Mesoscopic spin-boson models of trapped ions. Phys. Rev. A **78**(1), 010101 (2008)
24. Raizen, M.G., Gilligan, J.M., Bergquist, J.C., Itano, W.M., Wineland, D.J.: Ionic crystals in a linear Paul trap. Phys. Rev. A **45**(9), 6493 (1992)
25. Remoissenet, M.: Waves called solitons: concepts and experiments. Springer Science & Business Media (2013)
26. Russell, F.M., Eilbeck, J.C.: Evidence for moving breathers in a layered crystal insulator at 300 K. Europhys. Lett. **78**(1), 10004 (2007)
27. Russell, F.M., Zolotaryuk, Y.O., Eilbeck, J.C., Dauxois, T.: Moving breathers in a chain of magnetic pendulums. Phys. Rev. B **55**(10), 6304–6308 (1997)
28. Savin, A.V., Zolotaryuk, Y.O., Eilbeck, J.C.: Moving kinks and nanopterons in the nonlinear Klein-Gordon lattice. Phys. D **138**(3), 267–281 (2000)